

## Metallic Fuel Design Space for Sodium Fast Reactors

Ryan Stewart, Todd S. Palmer

*Radiation Transport and Reactor Physics Group, Oregon State University, 1500 SW Jefferson St. Corvallis, OR 97331, stewryan@oregonstate.edu*

### INTRODUCTION

Sodium fast reactors have received renewed attention for inclusion in the next generation of nuclear reactors [1]. This attention has been generated by government agencies and private companies looking to create alternative designs to traditional light water reactors [2, 3]. To successfully license and deploy these new reactor types, a thorough understanding of the fuel composition's impact on parameters such as fuel loading, reactor kinetics, and feedback mechanisms is required. There has been a focus on oxide cores in recent history, but many early sodium fast reactor (SFR) designs utilized metallic fuel [4, 5, 6]. Metallic fuel offers benefits over oxide fuel in terms of accident tolerance, as seen by tests performed at the Experimental Breeder Reactor II (EBR-II) [7]. The fuel density is typically higher in metallic fuels, which accommodates smaller core sizes, and metallic fuel can be reprocessed into new fuel with smaller facilities.

Sodium fast reactors contain higher levels of fissile material than their light water reactor counterparts. It is common to use a combination of enriched uranium and plutonium as fuel to decrease fuel loading and core size. No fast reactor to date has used plutonium as driver fuel and it will be important to understand the implications of changing fissile isotopes. This paper investigates the impact of plutonium fuel composition on various reactor parameters.

### BACKGROUND

To explore the design space for metallic fuels, five parameters were examined;  $k_{eff}$ ,  $\beta_{eff}$ , neutron generation time, the coolant void coefficient, and the Doppler coefficient.  $k_{eff}$  is an indicator of core fuel loading.  $\beta_{eff}$ , neutron generation time, the coolant void coefficient, and the Doppler coefficient impact reactor kinetics and feedback mechanisms which are integral to reactor safety. These quantities are important indicators of the design space for reactor neutronics and will help guide future reactor modeling.

The chosen metallic fuel base composition follows historical convention and consists of 90 wt% fuel, and 10 wt% zirconium. Zirconium is selected as an alloying agent due to past success in SFRs [8]. Six different fuel compositions with varying uranium enrichment and plutonium content were considered. Weapons grade plutonium isotopes are assumed in all plutonium compositions due to the lack of accessible reactor grade plutonium in the United States. Weapons grade plutonium is typically greater than 93 wt% Pu-239, and an arbitrary value of 94 wt% Pu-239 and 6 wt% Pu-240 was chosen for examination [9]. The Pu/U-235 ratio is allowed to vary, under the constraint that the sum of their weight fractions must equal 27 wt% of the total fuel. These various compositions can be seen in Table I.

TABLE I. Fuel Composition

	Pu (wt%)	U-235 (wt%)	U-238 (wt%)
27Pu	27.00	0.19	62.81
20Pu-7U	20.00	7.00	63.00
15Pu-12U	15.00	12.00	63.00
10Pu-17U	10.00	17.00	63.00
5Pu-22U	5.00	22.00	63.00
27U	0.00	27.00	63.00

### MODEL

Two different models were examined in this study. A single fuel assembly was modeled to draw initial conclusions about the material design space for metallic fuel. It was hoped that a single fuel assembly could provide accurate correlations and take less time to obtain results. These results could be used to provide a basis for full core modeling, without having to determine full core parameters such as control rod placement, number of radial reflectors, and experimental positions. This approach has been taken previously for fast reactor assemblies to determine burnup and sensitivity coefficients [10, 11]. In addition, full core models were created for each material composition and used to verify trends found in the single fuel assembly analysis.

All models were created and simulated in MCNP6 [12], and used cross-sections from the ENDFVII.1 library at 900 K. This temperature closely resembles typical operating conditions for SFRs (650 C). In the single assembly models, reflecting boundaries were placed on all radial sides, to simulate adjacent assemblies, while vacuum boundaries were used on the top and bottom. For  $k_{eff}$ ,  $\beta_{eff}$ , and the neutron generation time only the fuel compositions were changed between consecutive simulations. The coolant void coefficient was computed by adjusting the sodium density to 0.1% of the nominal density to simulate a core which has undergone a loss of coolant accident. Equation 1 was then used to find the coolant void coefficient. The Doppler coefficient was found performing calculations with cross-sections evaluated at 600 K and comparing with results from 900 K. Equation 2 was then used to find the Doppler coefficient.

$$\alpha_{void} = \frac{\Delta\rho}{\Delta\%_{void}} \quad (1)$$

$$\alpha_f = \frac{\Delta\rho}{\Delta T} \quad (2)$$

Each assembly consisted of four sections, as shown in Figure 1. The dark blue sections are the upper and lower reflectors consisting of 70 wt% HT-9 stainless steel and 30 wt% sodium. The yellow section is the plenum which consists of 25 wt% HT-9 stainless steel, 50 wt% sodium, and 25 wt% void.

The fuel region consists of 271 fuel pins, shown in orange, in a hexagonal lattice. The fuel pin height, diameter, and pitch are fixed at 60.0 cm, 0.395 cm, and 0.661 cm respectively. The fuel smear density (fractional area inside the inner cladding which is taken up by fuel) was maintained at 0.75. Where the fuel smear density can be used to yield the fuel diameter via:

$$R_{fuel} = \sqrt{\%A_{fuel}R_{IC}} \quad (3)$$

Where the  $R_{fuel}$  is the fuel radius,  $R_{IC}$  is the inner clad radius, and  $\%A_{fuel}$  is the fuel smear density. Surrounding each fuel pin is a homogenized representation of the HT-9 stainless steel wire wrap (17 wt%) and sodium coolant (84 wt%), shown in green. The inner duct flat-to-flat distance is 11.1 cm, with a duct thickness of 0.3 cm. The total height of the assembly is 220 cm, with each reflector section measuring 50 cm, and the plenum measuring the same height as the fuel region. The purple outline is the HT-9 stainless steel assembly duct.

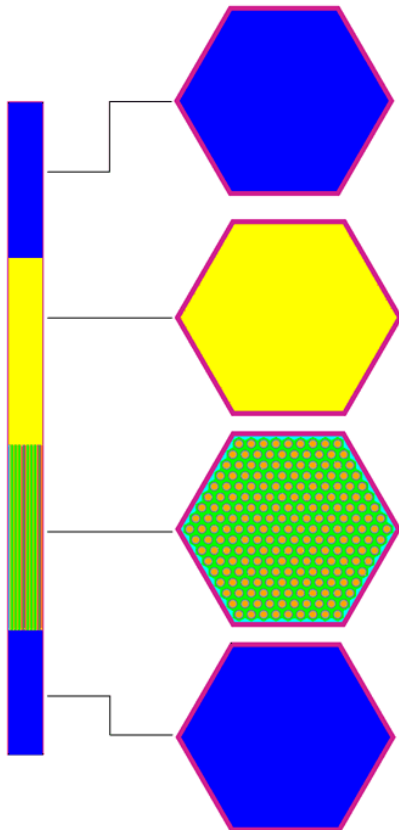


Fig. 1. Assembly Cross-Section

The full core model contains 78 fuel assemblies and is surrounded by approximately 40 cm of 30 wt% sodium and 70 wt% HT9 reflector. An additional 50 cm of sodium and 10 cm of HT9 are included above and below the core. Six control rod and two safety rod positions were included but withdrawn and replaced with a 90 wt% sodium 10 wt% HT9 mixture. Four positions contained the same mixture and were left as experimental positions. The full core model is shown Figure 2. The control rod and experimental positions can be

seen in pink, the fueled assemblies in green, the surrounding interstitial sodium in blue, and the reflector region in purple. The reflector region consists of a smear of HT9 (70 wt%) and sodium (30 wt%).

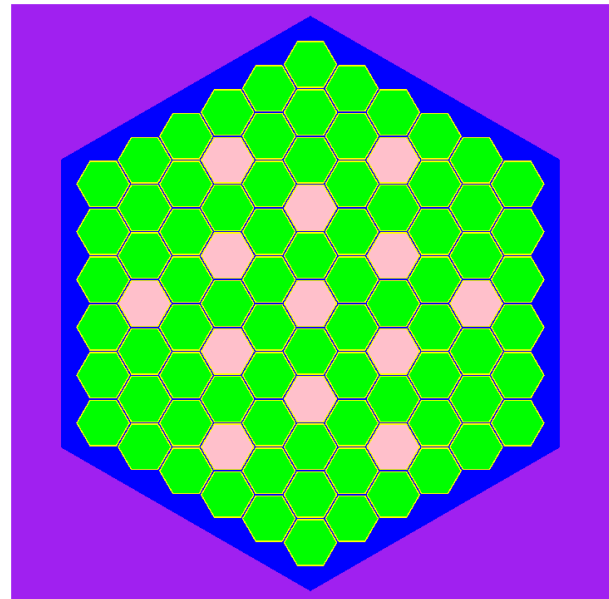


Fig. 2. SFR Full Core

**RESULTS**

Six MCNP6 simulations were completed using both the single assembly and full core models to examine the impact on  $k_{eff}$ ,  $\beta_{eff}$ , and the neutron generation time. The standard deviation in  $k_{eff}$  was less than 4 pcm, for  $\beta_{eff}$  the standard deviation was between 0.00004 - 0.00007, and for the neutron generation time ( $\Lambda$ ) the standard deviation was between 1.0 - 2.1 ns. The results of these simulations for the single assembly and full core analysis are shown in Table II and Table III.

TABLE II. Material Impact on  $k_{eff}$ ,  $\beta_{eff}$ , and Neutron Generation Time for a Single Assembly

Composition	$k_{eff}$	$\beta_{eff}$	$\Lambda$ (ns)
27Pu	1.67261	0.00272	159
20Pu-7U	1.59206	0.00361	179
15Pu-12U	1.53573	0.00427	195
10Pu-17U	1.47904	0.00509	214
5Pu-22U	1.42155	0.00582	235
27U	1.36378	0.00689	260

For the single assembly, there is a positive linear response in  $k_{eff}$  with respect to the plutonium fuel content and a negative linear response in  $\beta_{eff}$  and the neutron generation time. This indicates that utilizing plutonium as fuel material can provide a smaller fuel loading, and in turn a more compact core. The ability to reduce the amount of fissile material and core size comes at the of cost quicker reactivity response times. From tables III and II the single assembly analysis

TABLE III. Material Impact on  $k_{eff}$ ,  $\beta_{eff}$ , and Neutron Generation Time for a Full Reactor Core

Composition	$k_{eff}$	$\beta_{eff}$	$\Lambda$ (ns)
27Pu	1.24882	0.00288	319
20Pu-7U	1.18697	0.00369	362
15Pu-12U	1.14408	0.00452	391
10Pu-17U	1.10119	0.00530	428
5Pu-22U	1.05747	0.00608	467
27U	1.01390	0.00723	513

overestimates  $k_{eff}$  and underestimates both  $\beta_{eff}$  and the mean generation time. It is important then to focus on the full core.

The results from the full core analyses follow the same general trends of the single-assembly fissile content loading and reactivity control results. A core driven with plutonium has over 15 times the excess reactivity of a uranium driven core.  $\beta_{eff}$  of a plutonium driven core is around 2.5 times smaller than a uranium core, and the neutron generation time is around 1.5 times smaller. These provide insight into the importance of closely monitoring the plutonium fuel content for fuel loading and reactor kinetics.

Quantifying the results into correlations provides a better representation of the impact for each parameter. Fitting a linear regression model to  $k_{eff}$  with respect to the plutonium content for the single and full core analysis, respectively, yields:

$$k_{eff,sa} = 3.083E - 01(Pu) + 1.364E01 \quad (4)$$

$$k_{eff,fc} = 2.344E - 01(Pu) + 1.014E01 \quad (5)$$

Where Pu is the plutonium percent of fissile material. Applying this fit yields  $R^2$  values of 1.0000 and 1.0000. Similarly, for  $\beta_{eff}$  a linear regression yields:

$$\beta_{eff,sa} = -4.113E - 04(Pu) + 6.688E - 03 \quad (6)$$

$$\beta_{eff,fc} = -4.312E - 04(Pu) + 7.000E - 03 \quad (7)$$

This fit yields  $R^2$  values of 0.9915 and 0.9893. For the neutron generation time a linear regression yields:

$$\Lambda_{sa} = -1.006E02(Pu) + 2.547E02 \quad (8)$$

$$\Lambda_{fc} = -1.920E02(Pu) + 5.046E02 \quad (9)$$

This fit yields  $R^2$  values of 0.9921 and 0.9894. Further analysis of plutonium and uranium content variation could provide additional insight into cores with varying fissile content.

Coolant voiding was examined by computing the difference in  $k_{eff}$  between sodium at nominal density, and sodium at 0.1% of nominal density. The standard deviation in  $k_{eff}$  was less than 4 pcm, and the results are shown in Table IV.

For a fissile content of 27 wt%, full core voiding provides negative feedback for all types of fuel composition. This provides confidence that fuel with less than 27 wt% fissile content in a similar core geometry will provide negative feedback for coolant voiding. The correlation between the plutonium weight percent and the coolant void coefficient can be fit with a linear regression:

$$\alpha_{void} = 6.005E01(Pu) - 1.135E02 \quad (10)$$

TABLE IV. Material Impact on Coolant Void Coefficient

Composition	$\frac{d\rho}{d\%_{void}}$
27Pu	-56.40
20Pu-7U	-68.04
15Pu-12U	-77.75
10Pu-17U	-88.85
5Pu-22U	-101.73
27U	-116.74

This fit yields an  $R^2$  value of 0.9870, where this relationship is only valid for the specific core analyzed. However, this equation could provide an initial understanding of plutonium's effect on the coolant void coefficient for similar cores. Further analysis could supply information to determine the core size and fissile content which would create a positive void coefficient.

The coolant void coefficient results from the single assembly model are not presented here. Leakage is a major effect on the multiplication factor of small SFR cores and contributes to a negative coolant void coefficient. The model for a single assembly included radial reflecting boundaries yielding results that are not physically meaningful.

The Doppler coefficient was found by changing the cross-section set between 900 K and 600 K. This artificially decreases the energy at which neutrons experience collisions. The standard deviation in  $k_{eff}$  was less than 4 pcm. The results from these simulations are presented in Table V.

TABLE V. Material Impact on the Doppler Coefficient

	$\frac{d\rho_{SA}}{dT}$	$\frac{d\rho_{FC}}{dT}$
27Pu	-0.2416	-0.3927
20Pu-7U	-0.2443	-0.4394
15Pu-12U	-0.2668	-0.4628
10Pu-17U	-0.2861	-0.4501
5Pu-22U	-0.3163	-0.4970
27U	-0.3007	-0.5245

Table V demonstrates a non-linear relationship between the plutonium content and Doppler reactivity. A higher order polynomial could be used in the future, but for consistency and ease of visualization a linear regression is used and yields:

$$\alpha_f = 9.470E - 03(Pu) - 3.853E - 01 \quad (11)$$

$$\alpha_f = 1.482E - 03(Pu) - 6.390E - 01 \quad (12)$$

Applying  $R^2$  yields values of 0.861 and 0.919 for the single assembly and full core analysis. Although a linear fit is only an approximate, it can provide correlations for a simplified understanding of temperature feedback during accident scenarios. This could be coupled with correlations regarding the coolant voiding coefficient, and/or thermal hydraulics simulations to predict the behaviour of fuel during loss of coolant or loss of power accidents. Similar to  $k_{eff}$ ,  $\beta_{eff}$ , and the neutron generation time, additional modeling could provide correlations over a wider range of plutonium concentrations.

## CONCLUSIONS

Full core and single assembly analyses of the impact of material composition for metallic SFR fuel provides insight into various reactor parameters. This insight can provide useful correlations between the plutonium content and core life or kinetics behavior. For  $k_{eff}$  there is a positive linear relationship with respect to plutonium concentration, where the inverse is true for  $\beta_{eff}$  and the neutron generation time. These correlations can provide quick, on the fly adjustments to optimize fuel materials for sodium cooled fast reactors. Additional simulations may help to develop better correlations for relating plutonium content and  $k_{eff}$  or  $\beta_{eff}$  for various fissile contents and fissile loadings. For this particular core geometry, there was a positive linear relationship between the plutonium content and the coolant void coefficient. The coolant void coefficient remained negative for all concentrations of plutonium up to 27 wt%. Further investigation into higher plutonium concentrations may yield information on the threshold for a positive coolant void coefficient. The Doppler coefficient was found to have a non-linear relationship with respect to the plutonium content. Increasing the plutonium content tended to drive the Doppler coefficient smaller, but it remained negative for all plutonium concentrations. Further investigations into different fuel temperatures, and higher fissile content could provide additional information for negative feedback mechanisms.

Single assembly analysis did not accurately represent the physics occurring for any of the reactor parameters. Despite this, the results from the single assembly could be used as bounding conditions for a typical SFR. For  $k_{eff}$  it provides a bounding case for core size.  $\beta_{eff}$ , the mean generation time, and the Doppler coefficient provide minimum values for reactor kinetics and Doppler feedback. While the derivatives of  $k_{eff}$  and  $\beta_{eff}$  with respect to Pu content were similar in the single assembly and full core, the derivative of the neutron generation time with respect to the Pu content for the full core was nearly twice that of the single assembly. The computational times to execute the single assembly and full core MCNP6 models were nearly identical, further justifying the preference for full-core modeling of the fast reactor physics.

With the current relationships for  $k_{eff}$ ,  $\beta_{eff}$ , the coolant void coefficient, and the Doppler coefficient the a core optimization problem could be undertaken. Combining these with additional correlations regarding fuel pin geometry, assembly/core geometry, and thermal hydraulic constraints could provide a framework for optimizing SFR core designs. This could simplify the core design process and reduce the number of iterations required to design a core. If various reactor parameters are input into an algorithm containing these correlations, optimized core templates could be constructed quickly, without the need to perform any Monte Carlo or deterministic simulations. With a template created, it would then be the job of reactor designers to fine tune the models to their specifications.

## REFERENCES

1. C. VENARD ET AL., "The ASTRID core at the end of conceptual design phase," Tech. Rep. IAEA-CN245-288, IAEA (2017).
2. S. SEN ET AL., "Preliminary Options Assessment of Versatile Irradiation Test Reactor," Tech. Rep. INL/EXT-16-40780, Idaho National Laboratory (2017).
3. C. AHLFELD ET AL., "Conceptual Design of a 500MWe Travling Wave Demonstration Reactor Plant," *Proceedings of ICAAP 2011* (2011).
4. J. BESS, *Evaluation of the Initial Isothermal Physics Measurements at the Fast Flux Test Facility, A Prototypic Liquid Metal Fast Breeder Reactor*, FFTF-LMFBR-RESR-001, International Reactor Physics Experiments Evaluation Project, 2015 ed. (2006).
5. K. YOKOYAMA and A. SHONO, *Japan's Experimental Fast Reactor JOYO MK-I Core: Sodium-Cooled Uranium-Plutonium Mixed Oxide Fueled Fast Core Surrounded by UO<sub>2</sub> Blanket*, JOYO-LMFBR-RESR-001, International Reactor Physics Experiments Evaluation Project, 2015 ed. (2006).
6. E. LUM ET AL., *Evaluation of Run 138B at Experimental Reactor II, A Prototypic Liquid Metal Fast Breeder Reactor*, EBR2-LMFBR-RESR-001, International Reactor Physics Experiments Evaluation Project (in press).
7. T. SOFU, "A review of inherent safety characteristics of metal alloy sodium-cooled fast reactor fuel against postulated accidents," *Nuclear Engineering and Technology*, **47**, 3, 227 – 239 (2015).
8. L. WALTER, "Thirty years of fuel and materials information from EBR-II," *Journal of Nuclear Materials*, **270**, 39–48 (1999).
9. *Nonproliferation and Arms Control Assessment of Weapons-Usable Fissile Material Storage and Excess Plutonium Disposition Alternatives*, Department of Energy (1997).
10. J. SHEPPARD, *EBR-II Fuel Depletion Analysis Utilizing SCALE6.1 TRITON, T6-DEPL Sequence*, Master's thesis, Idaho State University (2016).
11. R. STEWART, C. POPE, and E. RYAN, "Fast spectrum reactor fuel assembly sensitivity analysis," *Annals of Nuclear Energy*, **110**, 1091–1097 (2017).
12. T. GOORLEY, "MCNP6 Release Overview," *Nuclear Technology*, **180**, 298–315 (2012).